**Journal of the Earth and Space Physics, Vol. 46, No. 4, Winter 2021, P. 117-129 (Research)**

**DOI:** 10.22059/jesphys.2020.296560.1007192

# Application of Forward and Inverse Modelling to High-Resolution Gravity Data for Mineral Exploration

Layade, G. O.[1*], Edunjobi, H. O.[2], Makinde, V.[3] and Bada, B. S.[1]

*1. Senior Lecturer, Department of Physics, College of Physical Sciences, Federal University of Agriculture, Abeokuta, Nigeria*

*2. M.Sc. Student, Department of Physics, College of Physical Sciences, Federal University of Agriculture, Abeokuta, Nigeria*

*3. Professor, Department of Physics, College of Physical Sciences, Federal University of Agriculture, Abeokuta, Nigeria*

*(Received: 27 Jan 2020, Accepted: 9 June 2020)*

## Abstract

Gravity survey is a geophysical tool used to investigate the subsurface by measuring the differences in Earth's gravitational field. The high-resolution gravity data within latitude $7^0.00^l$ - $7^0.30^l$ N, and longitude $3^0.00^l$ - $3^0.30^l$ E was acquired through Bureau Gravimetrique Internationale (EGM2008). The research work employed the methods of the filtering techniques as well as forward and inverse modelling for data analysis and interpretations. The qualitative results of the gravity anomaly of the field through the regional-residual separation technique and the high pass filters show the local and geologic features of the study area. The low, fairly high and high-density areas are characterized by alluvial, meta-sediments/sedimentary and igneous deposits respectively. The derivative maps aided the locations, boundaries and edges of anomalous bodies, including the transition zones and sedimentary intrusions of the study area. Forward and inverse modeling techniques were applied to profiles (P1-P4) in a quantitative approach, to describe the geometry, density contrast, depth, position, strike, dip and plunge. The depth range of 1268 m to 3111 m was calculated, while the density contrasts of gravity bodies suggest the presence of mineral rocks such as limestone, quartz, gneiss, sandstone, schist, granite, quartzite and gypsum.

**Keywords:** Gravity, Density, Filtering, High-resolution, Modelling, Depth.

## 1. Introduction

Geophysical surveying, although sometimes prone to some ambiguities and uncertainties of interpretations, provides a relatively rapid and cost-effective means of getting information about the sub-surface geology (Keary and Brooks, 1984). Gravity survey method is a non-destructive geophysical technique that measures differences in the Earth's gravitational field on different points at a specific location (Barnes et al., 2011; Nicolas, 2009).

In geosciences, the gravity survey method has been widely used in different applications like the regional and large scales of geophysical structures and engineering exploration. Gravity survey can be ground or airborne survey, in which measurements of the Earth's gravitational field are used to map the subsurface variations in density (Dransfield and Zeng, 2009; While et al., 2008)

Gravity and Magnetic survey methods are grouped together as Potential Field Methods, but there are basic differences between them; gravity is an inherent property of mass while the magnetic state of matter depends on factors like the inducing fields and the orientation of magnetic domains (Telford et al., 1976; Blakely, 1995; Mendonca and Silva, 1995; Adegoke and Layade, 2019).

Interpretation of gravity data is generally qualitative in the first stage, as there must be separation of anomalies before quantitative interpretation (Hammer, 1939; Pajot et al., 2008). Quantitative interpretation involves the description of the survey results and the explanation of the major features revealed by a survey in terms of the types of likely geological formations and structures that give rise to the evident anomalies (Revees, 2005). This information is geared towards mapping surface and subsurface structures such as intrusive rocks and outcrops.

Hence, the objective of this study is to investigate the parameters of causative anomalies (the possible type of geological feature/structure describing the area) that yielded the gravity field for mineral exploration within the Abeokuta area of Nigeria.

### 1-1. Theory of Gravitation

Newton's law of gravitation is the theory of all gravitational studies, which explains the

*Corresponding author: layadeoluyinka018@gmail.com

mutual attraction between two masses (**$m_1$** & **$m_2$**) separated by distance '**r**'.
If '**F**' is the force of attraction, then

$$F \alpha \frac{m_1 m_2}{r^2} \quad (1)$$

$$F = G\frac{m_1 m_2}{r^2} \quad (2)$$

where '*G*' is the universal gravitational constant taken to be 6.670 x $10^{-11}$ $Nm^2kg^{-2}$

$$F = mg \quad (3)$$

If $M_E$ represents the mass of the Earth and 'm' is the mass of a body located on the Earth's surface separated by distance 'r' from the Centre of the Earth, then, Equation (2) becomes:

$$F = G\frac{M_E m}{r^2} \quad (4)$$

Equating Equations (3) and (4) to have:

$$F = mg = G\frac{M_E m}{r^2}$$

$$g = G\frac{M_E}{r^2} \quad (5)$$

Equation (5) is the gravitational field of the Earth on any object within its sphere of influence. Thus, gravitational field of the Earth is expressed as the force per unit mass of any object on the surface of the Earth.

## 1-2. Location and Geology of the study area

The study area comprises of two geological formations of basement complex (Abeokuta formation) and sedimentary (Ewekoro) formations that is within latitude $7^0.00^I$ N to $7^0.30^I$ N and longitude $3^0.00^I$ E to $3^0.30^I$ E, covering an area of about 3025 $km^2$. According to Rahaman (1976), the gneiss-migmatite complex is the mostly widespread rock formation within Abeokuta and comprises of quartzite, calcsilicate, gneisses, amphibolites and biotite-hornblende schist. According to Jones and Hockey (1964), the older granites in the Abeokuta area are of Precambrian age to early Paleozoic age and are magmatic in nature.
The location falls within the basement complex of the geological setting of south western Nigeria (Obaje, 2009). Abeokuta is bounded in the South, North, East and West by Lagos, Oyo/Osun, Benin Republic and Ondo State respectively (Figure 1).

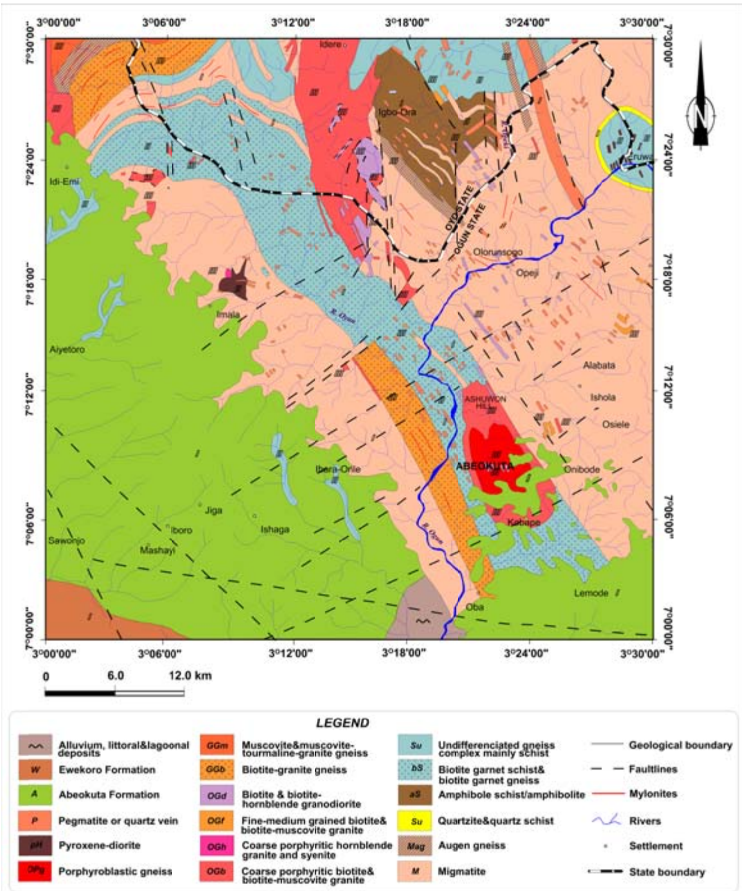


**Figure 1.** Geological Map of the Study Area.

## 2. Methodology

### 2-1. Data Acquisition

The Bouguer gravity data acquired by Bureau Gravimetrique Internationale (BGI) through Earth Gravity Model (EGM2008) satellite in 2008 was used in this research. The data contained the longitude, latitude and the corrected gravitational field variations (Bouguer gravity values).

### 2-2. Data Processing Techniques

The research data were analyzed using both qualitative and quantitative methods. The gravity dataset of the study area was prepared, processed, analyzed and interpreted using Oasis Montaj Software (version 7.5) and PotentQ Modelling software. The dataset in x, y and z columns, which correspond to the longitude, latitude and depth, respectively the density contrasts (in mGal) is converted into grid using the minimum curvature gridding tool of Oasis Montaj.

The grid produced, yielded the Bouguer gravity anomaly map of the area and environs. Regional-residual separation was performed on the Bouguer gravity map through polynomial fitting of the first order to produce the residual anomaly (Reynolds, 1997; Houghton et al., 2007). The shorter wavelength (residual) anomaly was filtered to produce the derivative grids (first and second vertical and horizontal derivative grids, analytic signal grid), through a one-dimensional fast Fourier transform (FFT1D) in order to enhance the anomalies associated with shallow sources (Zahra and Hesham, 2016).

The vertical derivative technique is based on the expression;

$$\mathcal{F}\left[\frac{d^n\phi}{dz^n}\right] = k^n\mathcal{F}(\phi) \tag{6}$$

where,

$\mathcal{F}$ = Fourier transform of the gravity field

$n$ = 1, 2, the n$^{th}$ order vertical derivative

$\phi$ = Potential of the gravity field

The horizontal derivatives of the potential field $\phi$(x,y) in the Fourier domain, in x and y directions can be given as;

$$\mathcal{F}\left[\frac{d^n\phi}{dx^n}\right] = (ik_x)^n\mathcal{F}(\phi) \tag{7}$$

and

$$\mathcal{F}\left[\frac{d^n\phi}{dy^n}\right] = (ik_y)^n\mathcal{F}(\phi) \tag{8}$$

($ik_x$) and ($ik_y$) are operators that transform a function into n$^{th}$ order derivatives with respect to x and y, respectively.

Direct and indirect (otherwise known as the forward and inverse modelling) method of qualitative analysis was employed using PotentQ modelling software. The forward modelling involves creating a model (a hypothetical source), calculating the gravity anomaly, comparing it with the observed data and adjusting the model until the data are well fit. The initial model was obtained by using the parametric measurements or the geological information of the area. The inverse modelling is concerned with calculating the parameters (nature) of the anomalous body by the computer automatically (Onyishi et al., 2019; Foulger et al., 2013). The contoured Bouguer anomaly grid was used for these methods and different regions (labelled P1-P4) of the area yielded the dimensions of their different anomalies respectively.

## 3. Results and Discussions

The Bouguer gravity data grid (Figure 2) was separated into regional (Figure 4) and residual (Figure 5) grids in order to enhance the information of the local features characterizing the study area. The regional grid (Figure 4) is herein treated as the noise that contains short frequency anomalies ranging from 12.86 mGal to 22.44 mGal.

Further enhancements were made on the residual grid, which consequently generated the first vertical and horizontal derivative grids (Figures 6 and 7), the derivative grids produced to show the locations, edges and boundaries of the gravity anomalous sources that yielded the field.

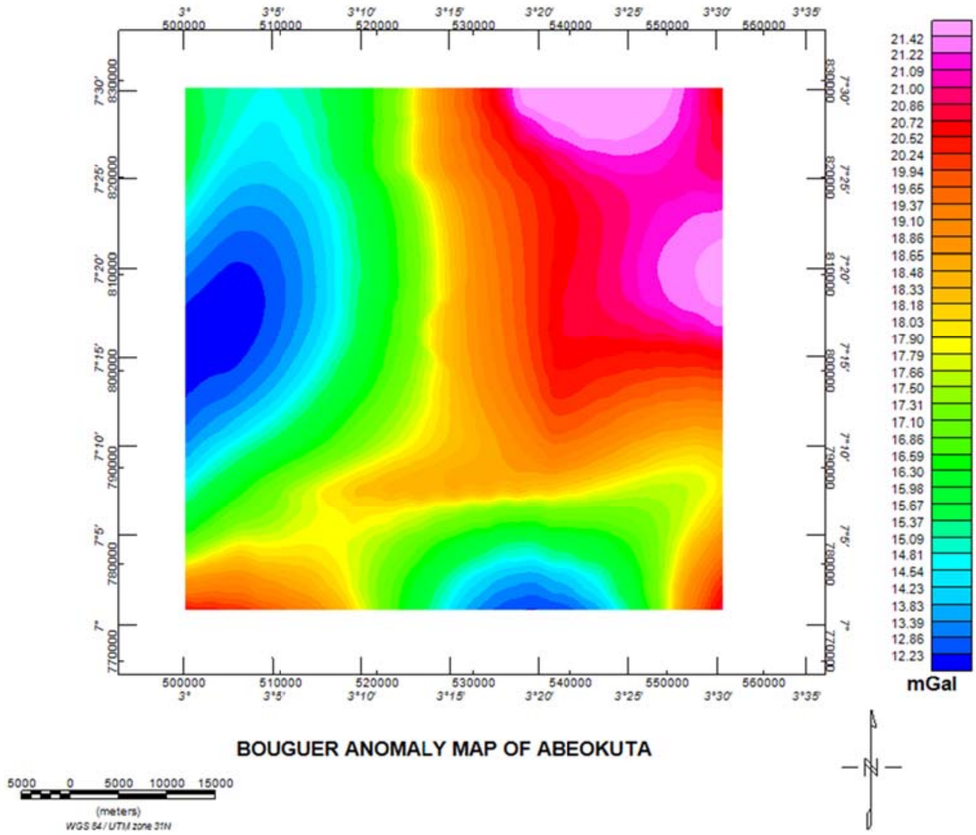


**Figure 2.** Bouguer Gravity Field of Abeokuta and Environ.

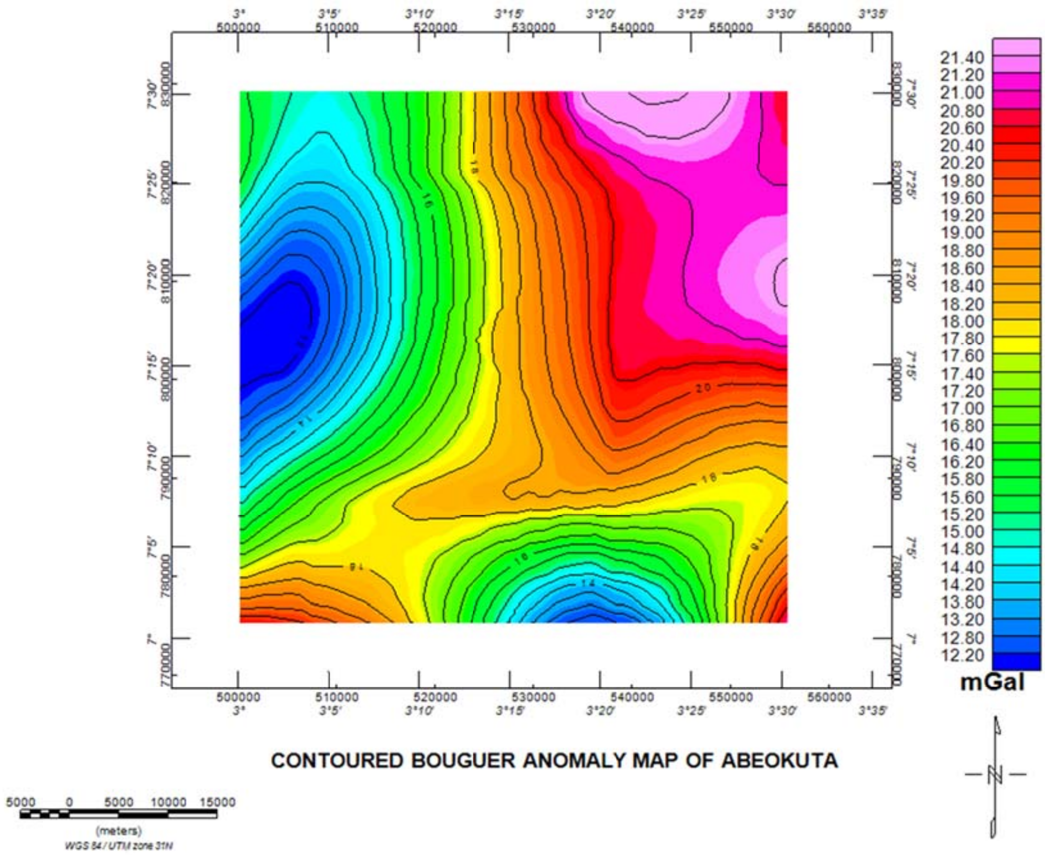


**Figure 3.** Contoured Bouguer Anomaly Field of Abeokuta and Environs (0.2 mGal interval).

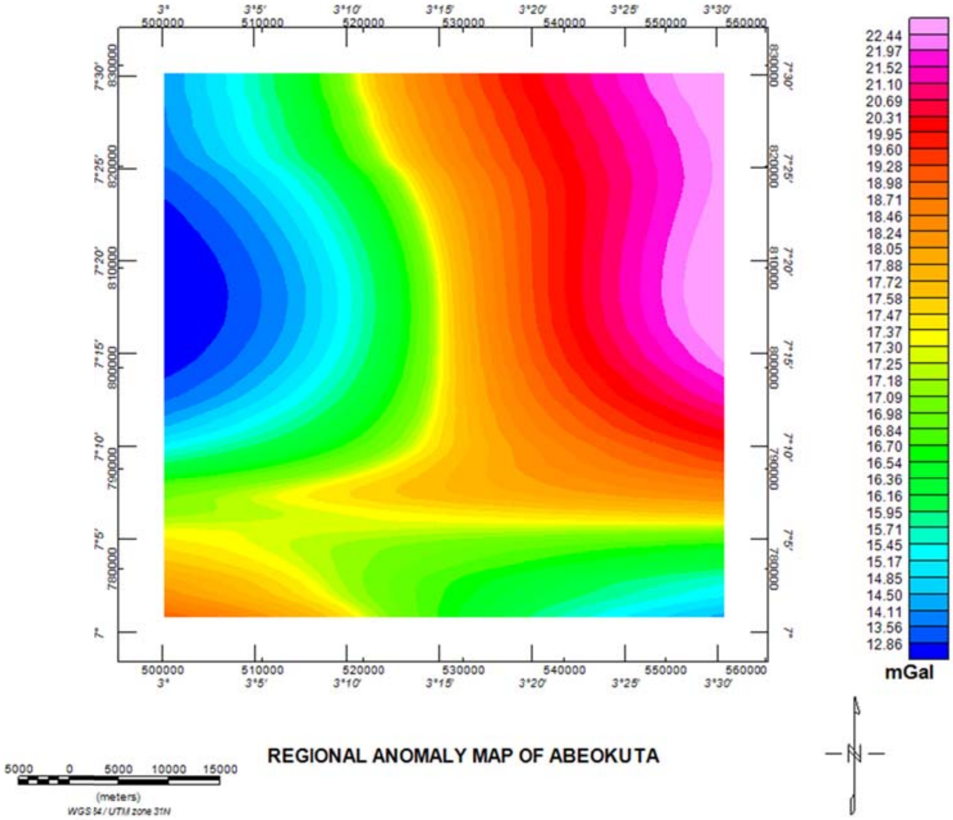


**Figure 4.** Regional Anomaly Field of Abeokuta and Environ.

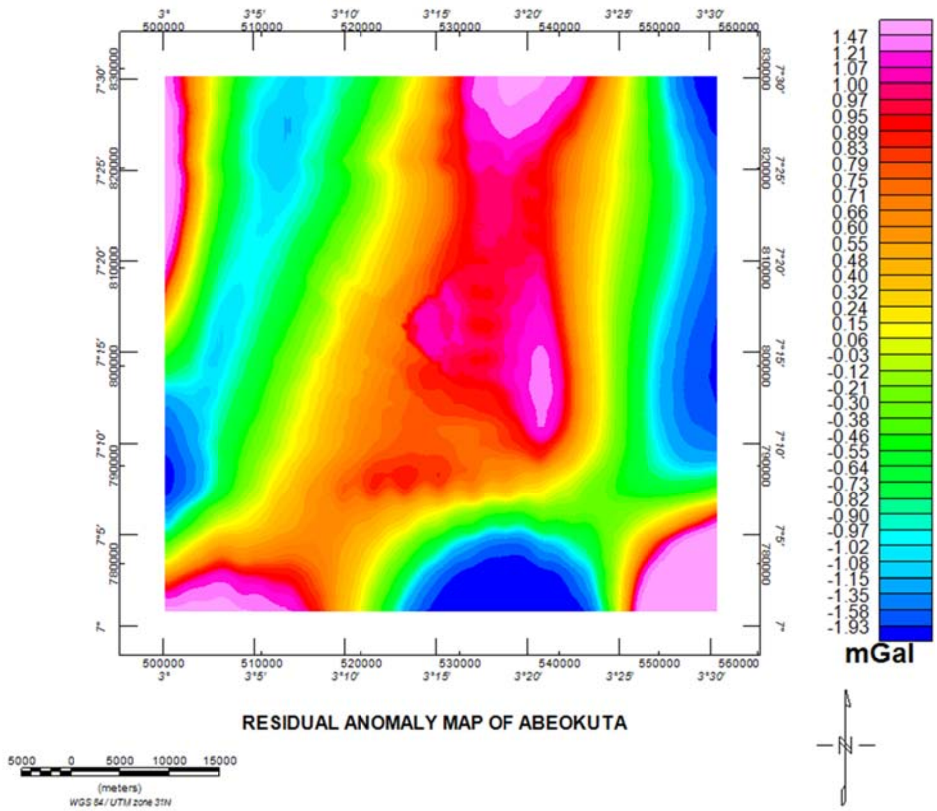


**Figure 5.** Residual Anomaly Field of Abeokuta and Environ (short wavelength anomalies).

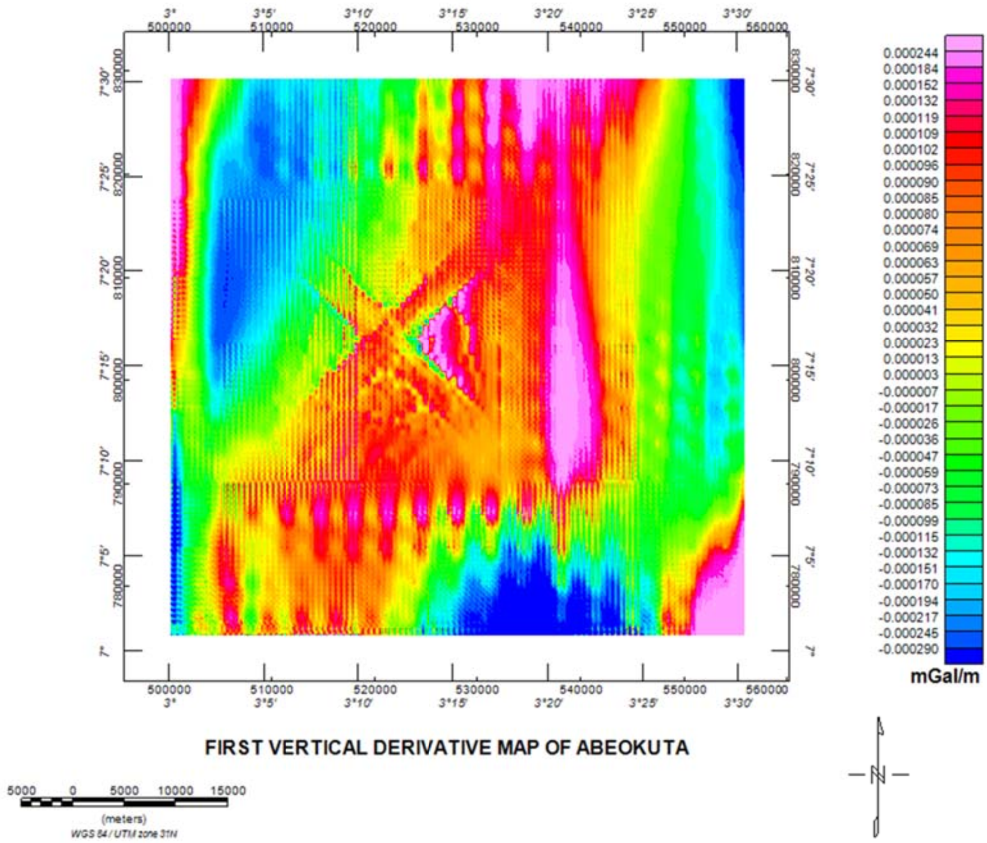


**Figure 6.** Vertical Derivative Map of the First Order of Abeokuta and Environ.

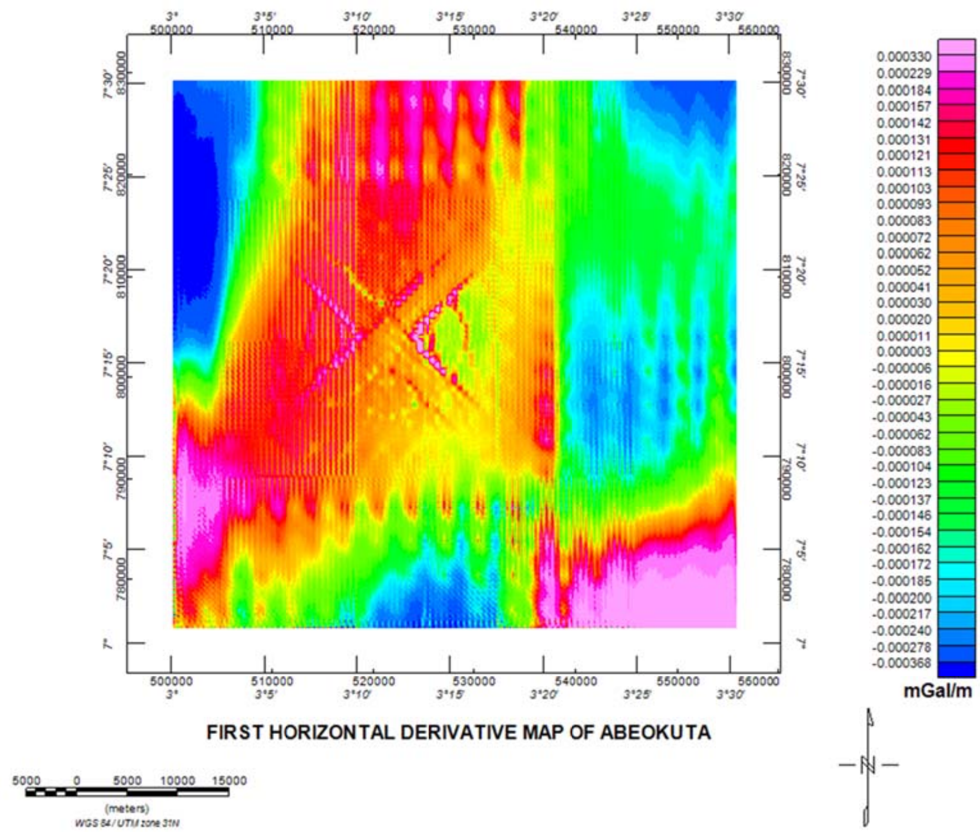


**Figure 7.** First Horizontal Derivative Map of the Study Area.

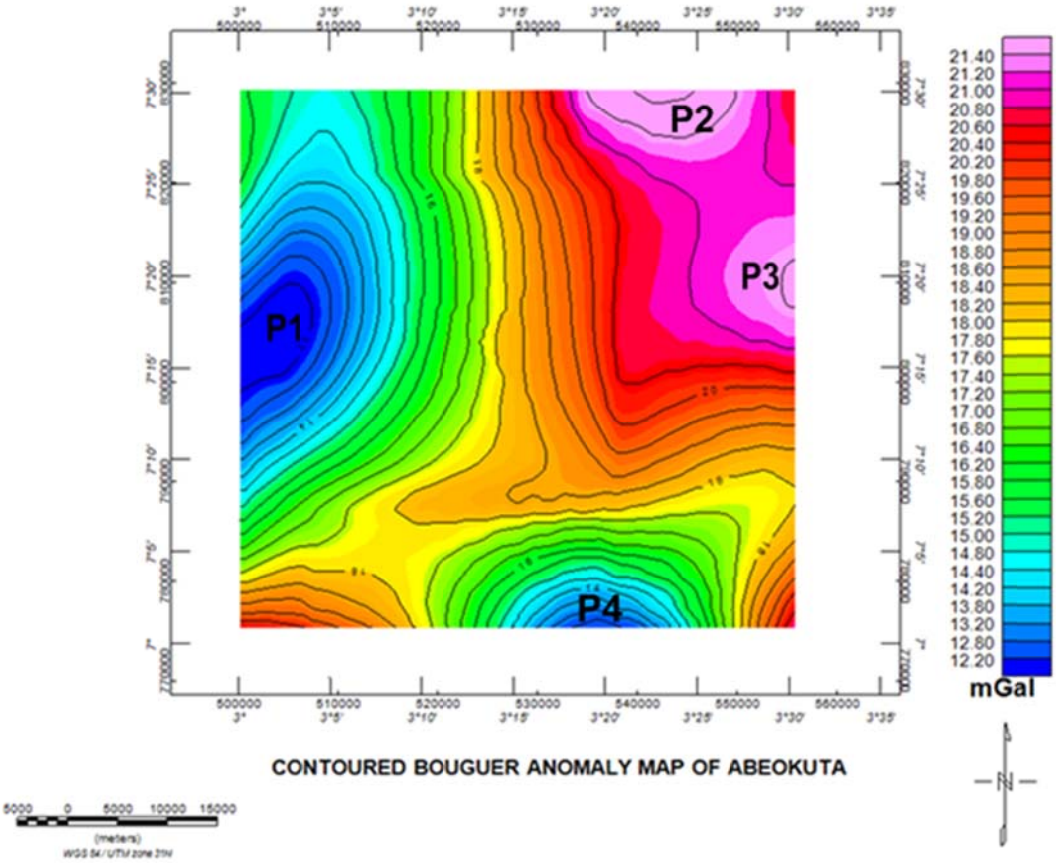


**Figure 8.** Contoured Bouguer Anomaly at 0.20 mGal interval, showing the Modelled Regions.

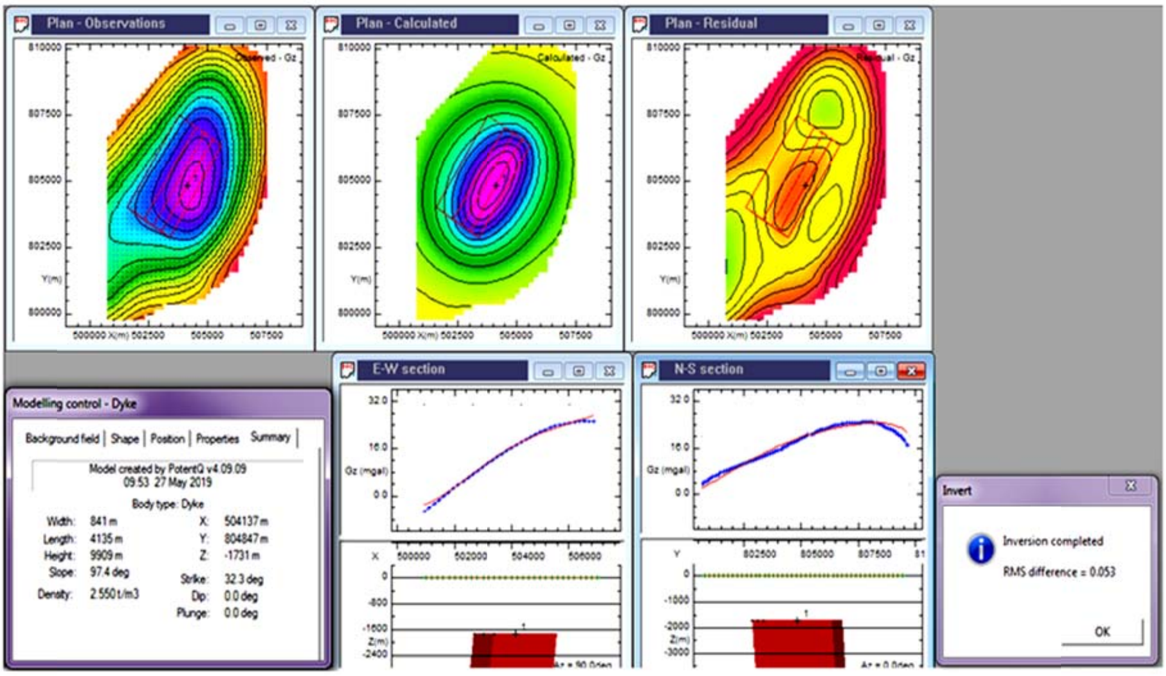


**Figure 9.** Forward and Inverse Modelling Result of Profile 1 (P1).

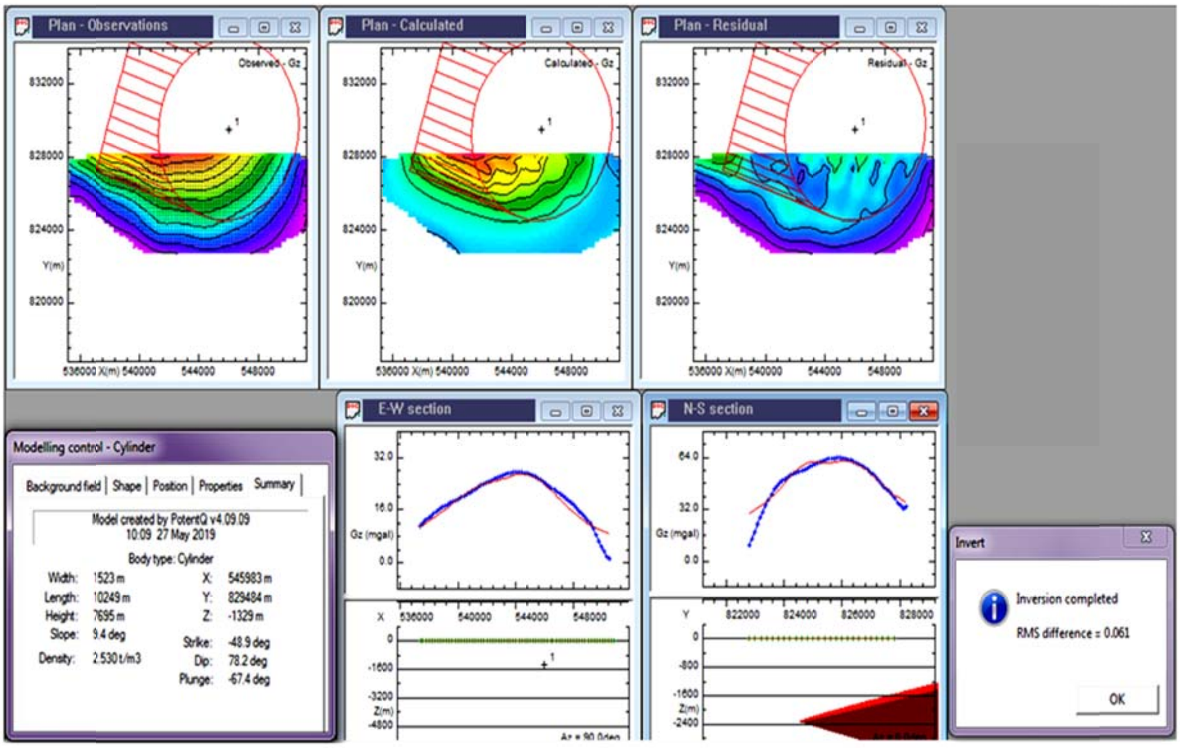


**Figure 10.** Forward and Inverse Modelling Result of Profile 2 (P2).

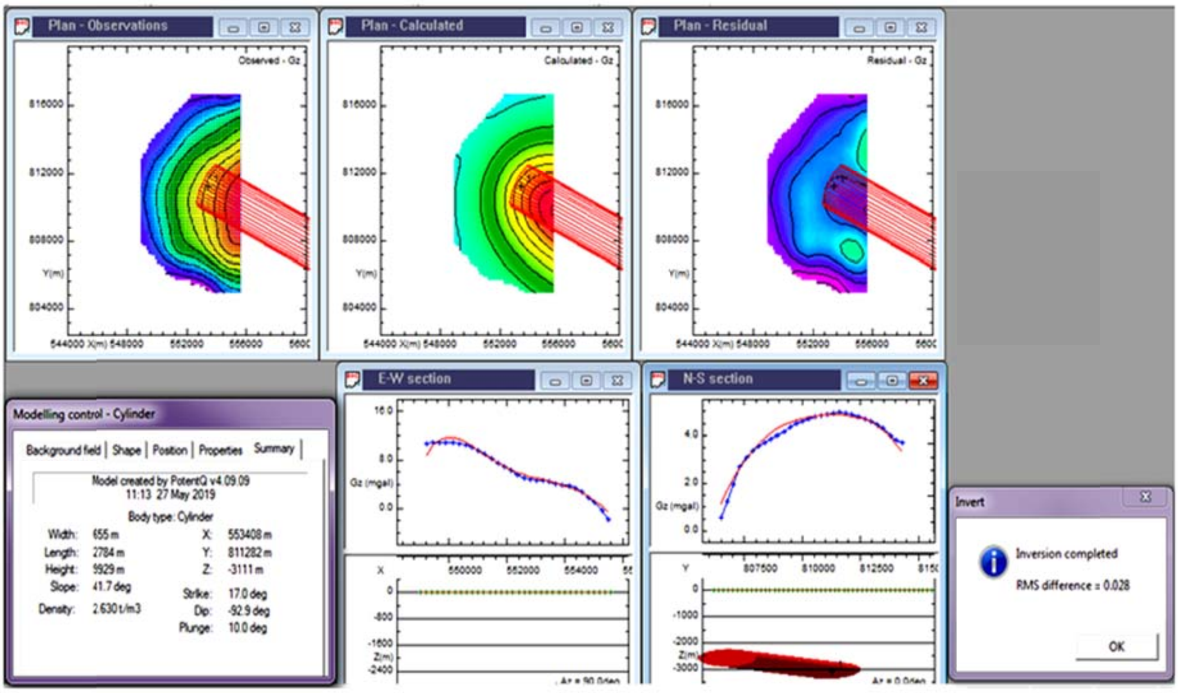


**Figure 11.** Forward and Inverse Modelling Result of Profile 3 (P3).

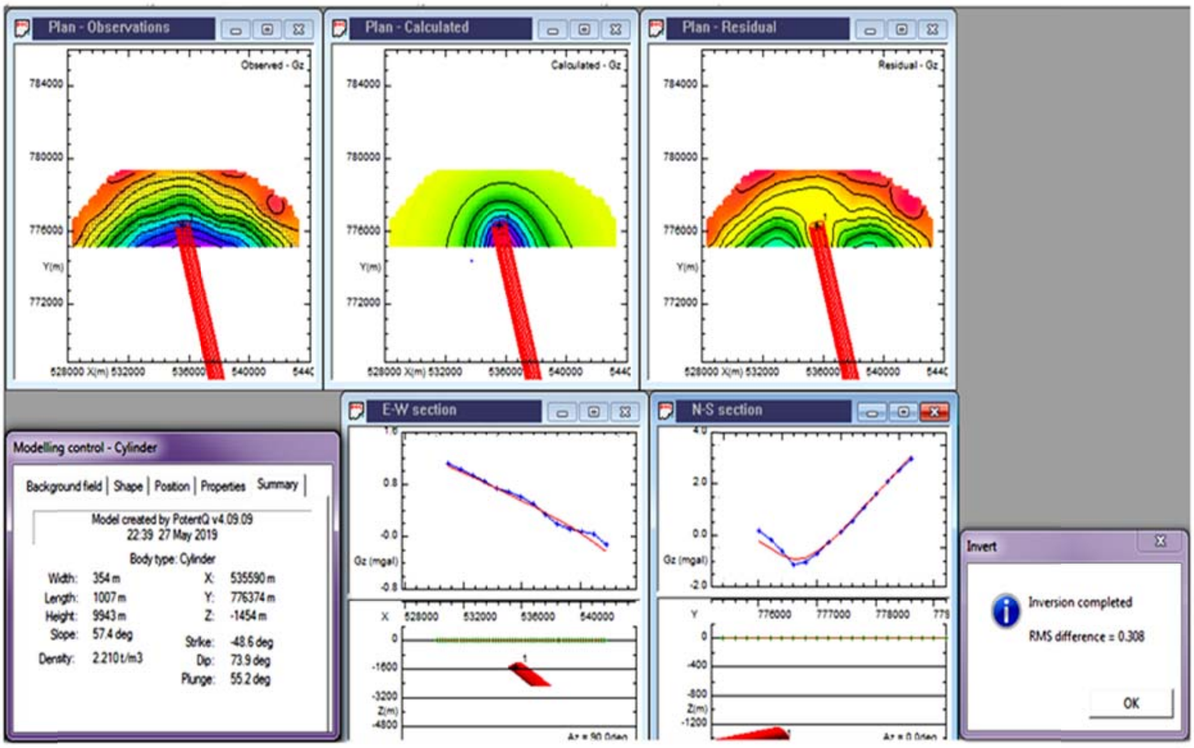


**Figure 12.** Forward and Inverse Modelling Result of Profile 4 (P4).

The study area as shown by the Bouguer gravity anomaly map (Figure 2) of Abeokuta and environ is characterized by three distinguishable features of: (i) gravity highs around the northeastern part, (ii) moderate gravity values trending NSN, SE-SW and partly at the northwestern region, and (iii) gravity lows around the southern, southwestern and northwestern portions of the study area. The high gravimetric values are related to the lithological variations in the basement while the low gravimetric values are related to the lithological variations intra-basement of the research area. The Bouguer anomaly field (Figure 2) reveals that the study area comprises of basement complex and sedimentary formation with transition zone, which is associated with basement, intra-basement and cultural sources.

Contoured Bouguer anomaly map (Figure 3) has a gravity range of 12.23 mGal to 21.42 mGal, the value range of 12.23 mGal to 15.10 mGal depicts the area of low density contrasts while the range of 20.53 mGal to 21.42 mGal defines the area with high density contrasts in the study area. The contoured Bouguer anomaly shows a cluster of long wavelength anomalies around the southern and northwestern parts of the area, the observed spaced contour pattern of anomalies around the northeastern and southwestern regions suggest that the anomalies in those areas are of deeper sources while the relatively closed contour pattern indicates anomalies of shallower sources.

The residual anomaly map (Figure 5) with a gravimetric range of -1.93 mGal to 1.47 mGal is the short wavelength anomalies of the Bouguer anomaly field, with its gravity highs majorly around the central zones, partly around the southeastern and southwestern regions of the study area. The observed faint high density contrasts around the southeastern and southwestern parts of the residual map (Figure 5) were as a result of the removal of long wavelength anomalies (i.e. the regional anomaly, referred to as the noise) obscuring the short wavelength anomalies (signal) from the Bouguer gravity field during separation. The low-density contrasts anomalies running through the southwestern to northwestern zones of the area are the sedimentary intrusions into the basement complex formation, which suggest possible deposits of lower density bodies like the alluvial deposits, limestone, shale, sandstone and the likes.

The derivative maps (Figures 6 and 7) are high pass filters that show the vertical and horizontal rate of change in the gravity field with depth. These were computed from the residual anomaly map (Figure 5) to attenuate the regional effects of the field thereby enhancing the shallow features. Comparing the derivative grids to the residual anomaly map, it can be clearly seen that local geological features are conspicuous and this is because the high pass filters have high sensitivity to gravity responses. The derivatives generally have lateral orientation of anomalies along N-S trend of the study area, which depicts homogeneity of anomaly sources.

The first vertical derivative map (Figure 6) has an anomaly range of -0.00029 mGal/m to 0.00024 mGal/m with high gravity sources at the northcentral and southeastern parts. The first horizontal derivative map (Figure 7) shows a horizontal displacement of bodies in the field, the gravitational field ranges from -0.00037 mGal/m to 0.00033 mGal/m with its high gravity values dominant at the north-central portion of the map. The first horizontal derivative map (Figure 7) also reveals some closely packed and loosely-spaced contours, which are possible fault zones and lineaments of the study area. The lineaments serve as entrapments and conduits for economic deposits.

The modelled regions of the Bouguer anomaly in Figure 8 were contoured at 0.20 mGal interval. From the forward and inverse modelling profiles (Figures 9 to 12), Profile 1 (P1) (Figure 9) is located at the southwestern portion of the study area that is within 800,000 m – 810,000 m Easting and 500,000 m – 507,500 m Northing, the gravity response possibly suggests a monocline in that region of the study area. The model is dyke with the density of the anomalous body to be 2.550 g/m$^3$ at a depth of 1,731 m.

Profile 2 (P2) (Figure 10), at an approximate position of 820,000 m – 832,000 m Easting and 536,000 m – 548,000 m at the northeastern part of the study area, whose gravity signature possibly describes an antiformal structure. The cylinder model shows an anomalous body of 2.530 g/m$^3$ at a vertical distance of 1,329 m at the subsurface. While Figure 11 revealed the third profile (P3), situated at 804,000 m – 816,000 m Easting and 544,000 m – 560,000m Northing. The gravity structure is possibly antiformal in nature, cylindrically modelled with an anomalous body of 2.630 g/m$^3$ density at a depth of 3,111 m.

The fourth profile 4 (P4) in Figure 12 is at the bottom southern region of the gravity field, which lies within 772,000 m – 784,000 m Easting and 528,000 m – 544,000 m Northing having a geologic structure that possibly describes a monocline. The model reveals an anomalous body with a density of 2.210 g/m$^3$ at 1,454 m depth.

Generally, the anomalous bodies in all profiles (P1-P4) have density of 2.550 g/cm$^3$, 2.530 g/cm$^3$, 2.630 g/cm$^3$ and 2.210 g/cm$^3$ respectively. These densities possibly suggest the presence of quartz, kaolinite, marble, limestone, sandstone, granite, quartzite, gneiss and other alluvial deposits in the study area, which are in agreement with the research carried out by Akinse and Gbadebo (2016) and Badmus et al. (2013) with aeromagnetic data. The depths of anomalous on the profiles 1, 2, 3 and 4 are 1,731 m, 1,329 m, 3,111 m and 1,454 m, respectively. The depths fairly agree to that of Olowofela *et al*. (2013), whose depth to magnetic basement range is 145 m – 2,692 m. The estimated depths are also close to the research studies carried out by Olurin *et al*., (2015), which employed three approaches of horizontal gradient method, local wave number method and analytical signal method, to yield depth ranges of 503 m – 2,340 m, 931 m – 4,900 m and 554 m – 2,490 m, respectively. This is in addition to the work done by Bello and Falano (2017), whose depth range is 1,047 m – 3,600 m in the study area.

**Table 1.** Ranges and averages of densities of common rocks (Telford et al., 1990).

| Rock | Density ($kgm^{-3}$) | |
|---|---|---|
| | Range | Average |
| **Sediments and Sedimentary rocks** | | |
| Sandstone | 1600 – 2760 | 2350 |
| Shale | 1560 – 3200 | 2400 |
| Limestone | 2040 – 2900 | 2550 |
| Halite | 2100 – 2600 | 2220 |
| Gypsum | 2200 – 2600 | 2350 |
| Coal | 1340 – 1800 | 1500 |
| Oil | 600 – 900 | - |
| **Igneous Rocks** | | |
| Sandesite | 2400 – 2800 | 2610 |
| Granite | 2500 – 2810 | 2640 |
| Basalt | 2700 – 3300 | 2990 |
| Gabbro | 2700 – 3500 | 3030 |
| Peridotite | 2780 – 3370 | 3150 |
| **Metamorphic Rocks** | | |
| Quartzite | 2500 – 2700 | 2600 |
| Schist | 2390 – 2900 | 2640 |
| Granulite | 2520 – 2730 | 2650 |
| Marble | 2600 – 2900 | 2750 |
| Slate | 2700 – 2900 | 2790 |
| Gneiss | 2590 – 3000 | 2800 |

**Table 2.** Summary of forward and inverse modelling results.

| Profiles | Model | Anomalous structure | Density ($g/m^3$) | Depth (m) | Plunge (deg) | Dip (deg) | Strike (deg) | Possible minerals |
|---|---|---|---|---|---|---|---|---|
| P1 | Dyke | Monocline | 2.550 | 1,731 | - | - | 32.3 | Limestone, Kaolinite, Quartzite |
| P2 | Cylinder | Antiform/anticline | 2.530 | 1,329 | -67.4 | 78.2 | -48.9 | Granite, Quartzite, Gypsum |
| P3 | Cylinder | Antiform/anticline | 2.630 | 3,111 | 10.0 | -92.9 | 17.0 | Schist, Gneiss, Quartzite, Quartz, Marble |
| P4 | Cylinder | Monocline | 2.210 | 1,454 | 55.2 | 73.9 | 48.6 | Clay, Sand, Gravel, Gypsum |

## 4. Conclusion

The study area was investigated using BGI gravity data to reveal the subsurface features, which includes the type, shape and depth of anomalous sources. Qualitatively, polynomial fitting and high pass filtering techniques were used to describe areas of high and low-density contrast values and the tectonic trends of gravity anomalous sources. The northeastern part of the area is associated with high-density bodies while the southern and northwestern regions comprise of low-

density bodies.
The detailed analysis and interpretation of the high-resolution gravity data carried out revealed that the area has prospect for mineral exploration as the preponderance of mineral rocks such as limestone, quartz, gneiss, sandstone, schist, granite, quartzite and gypsum were evident.

**Acknowledgement**
The Authors are grateful to Bureau Gravimetrique Internationale (BGI) for providing the gravity data used in this research.

**References**

Adegoke, J. A. and Layade, G. O., 2019, Comparative depth estimation of iron-ore deposit using the Data-Coordinate Interpolation Technique for airborne and ground magnetic survey variation, African Journal of Science, Technology, Innovation and Development. 11(5), 663-669, doi: 10.1080/20421338.2019. 1572702.

Akinse, A.G. and Gbadebo, A.M., 2016, Geological mapping of Abeokuta Metropolis, Southwestern Nigeria. International Journal of Scientific & Engineering Research, 7(8), 979-983.

Badmus, B.S., Olurin, O.T., Ganiyu and, S.A. and Oduleye, O.T., 2013, Evaluation of Physical Parameters of Various Solid Minerals within Southwestern Nigeria using Direct Experimental Laboratory Methods. American International Journal of Contemporary Research, 3(3), 152-161.

Barnes, G. J., Lumley, J. M., Houghton P. and Gleave, R., 2011, Comparing gravity and gravity gradient surveys: Geophysical Prospecting, 59, 176–187, doi:10.1111/j.1365-2478.2010.00900.x.

Bello, R. and Falano, O.C., 2017, Interpretation of Aeromagnetic Anomalies over Abeokuta, Southwest Nigeria, using Spectral Depth Technique. Journal of Applied Sciences in Environmental Management, 21(2), 218-222.

Blakely, R. J., 1995, Potential theory in gravity and magnetic applications: Cambridge University Press. ISBN: 9780511549816; DOI: 10.1017/CBO9780511549816.

Dransfield, M. H. and Zeng, Y., 2009, Airborne gravity gradiometry: Terrain corrections and elevation error. Geophysics, 74, I37-I42.

Foulger, G.R., Du, Z. and Julian, B.R., 2013, Icelandic Type Crust, Geophysical Journal International, 155, 567-590.

Hammer, S., 1939, Terrain corrections for gravimeter stations: Geophysics, 4, 184–194, doi:10.1190/1.1440495.

Zahra, H.S. and Hesham, T.O., 2016, Application of High-Pass Filtering Techniques on Gravity and Magnetic Data of the Eastern Qattara Depression Area, Western Desert, Egypt. National Research Institute of Astronomy and Geophysics, 5, 106-123.

Houghton, P., Bate, D., Davies, M. and Lumley, J., 2007, Using gravity gradiometry as a blueprint for exploration in thrust and fold belts: First Break, 25, 105–112.

Keary, P. and Brooks, I., 1984, Introduction to Geophysical Exploration. Blackwell Scientific Publishers, in: Pure Appl. Geophys, 123(1985), 171–172.

Jones, H.A. and Hockey, R.O., 1964, The Geology of Parts of Southwestern Nigeria. Bull. Geol. Surv. Nigeria 31, 101 – 102.

Mendonca, C. A. and Silva, B. C., 1995, Interpolation of potential-field data by equivalent layer and minimum curvature: A comparative analysis: Geophysics, 60, 399–407, doi:10.1190/1.1443776.

Nicolas, O.M., 2009, The Gravity Method. Exploration for Geothermal Resources, 1-9.

Obaje, N.G., 2009, Geology and mineral resources of Nigeria. Lecture Note in Earth Science Series, Vol. 120.

Onyishi, G.E., Ugwu, G.Z. and Okonkwo, A., 2019, Forward and Inverse Modelling of Aeromagnetic Anomalies over Parts of Middle Benue Trough, Nigeria. American Journal of Geophysics, Geochemistry and Geosystems, 5(1) 16-23.

Olowofela, J.A., Akinyemi, O.D., Badmus, B.S., Awoyemi, M.O., Olurin, O.T. and Ganiyu, S.A., 2013, Depth estimation and source location of Magnetic anomalies from a Basement Complex Formation, using Local Wavenumber Method (LWM). IOSR Journal of Applied

Physics, 4(2), 33-38.

Olurin, O.T., Olowofela, J.A., Akinyemi, O.D., Badmus, B.S., Idowu, O.A. and Ganiyu, S.A., 2015, Enhancement and Basement Depth Estimation from Airborne Magnetic Data. African Review of Physics, 10(38), 303-313.

Pajot, G., de Viron, O., Diament, M., Lequentrec-Lalancette, M.F. and Mikhailov, V., 2008, Noise reduction through joint processing of gravity and gravity gradient data: Geophysics, 73(3), I23–I34, doi:10.1190/ 1.2905222.

Rahaman, M.A., 1976, Review of the basement geology of south western Nigeria in Geology of Nigeria edited by C. A Kogbe. Elizabethan publishing company, Lagos; 41-58.

Revees, C., 2005, Aeromagnetic Surveys; Principles, Practice and Interpretation. GEOSOFT, 155.

Reynolds, M.J., 1997, Introduction to applied and environmental geophysics. John Wiley and Sons, New York USA. 796 p.

Telford, W. M., Geldart, L. P., Sheriff, R. E. and Keys, D. A., 1976, Applied Geophysics: Cambridge University Press. xvii + 860 pp.

Telford, W.M., Geldart, L.P. and Sheriff, R.E., 1990, Applied geophysics (2nd edition), Cambridge University Press, Cambridge, 770.

While, J., Biegert, E. and Jackson, A., 2008, Interpolation of gravity and gravity gradient data by using the generalized sampling expansion: Theory: Geophysics, 73(2), I11–I21, doi:10.1190/1.2831934.